

Cite this: *Chem. Commun.*, 2012, **48**, 5449–5451

www.rsc.org/chemcomm

COMMUNICATION

A fluorescence turn-on H₂O₂ probe exhibits lysosome-localized fluorescence signals†Dayoung Song,^a Jung Mi Lim,^b Somin Cho,^a Su-Jin Park,^b Jaeheung Cho,^a Dongmin Kang,^b Sue Goo Rhee,^b Youngmin You*^a and Wonwoo Nam*^a

Received 5th March 2012, Accepted 3rd April 2012

DOI: 10.1039/c2cc31632c

A new fluorescence turn-on probe that responds exclusively to H₂O₂ exhibits subcellular localized fluorescence staining of lysosomes.

Hydrogen peroxide (H₂O₂) plays a crucial role in many biological processes in the human body, including respiration,¹ intracellular signalling,² and immune responses.^{3,4} Despite the intense investigation over the past several decades, the chemical mechanisms of the H₂O₂-mediated processes have not been fully established yet. Thus, the elucidation of these processes would benefit from the development of sensors capable of identifying and monitoring the trafficking and localization of intracellular H₂O₂.^{5,6} Fluorescence probes are appropriate for this application since fluorescence signals exhibit excellent spatial resolution, fast response times, and high signal-to-noise ratios. These benefits have been exploited in the development of fluorescent H₂O₂ probes based on chemical reactions with H₂O₂,⁷ including oxidation of phosphine,⁸ dihydrodichlorofluorescein,⁹ dihydrorhodamine,¹⁰ and dihydrophenoxazine.¹¹ In addition, H₂O₂-induced cleavage of boronate,¹² arylsulfonyl,^{13,14} benzyl,¹⁵ *p*-aminophenol,¹⁶ and hydroquinone¹⁶ has been employed as a viable means for turning on fluorescence signals by H₂O₂. Chelation of H₂O₂ by a Eu³⁺-tetracycline complex has also been evaluated as a means for fluorescent detection.¹⁷ Although some of these probes have permitted the detection and quantification of intracellular H₂O₂, such probe systems lack full applicability to biological systems due to modest selectivity, requirements for external enzymes, slow response time, or incompatibility with biological milieus.

An alternative approach to fluorescent H₂O₂ detection is the mimicking of bioredox processes between H₂O₂ and metallo-enzymes, such as the interaction between iron porphyrin centers of heme enzymes and H₂O₂, which catalyzes the oxidation of a wide variety of biological substrates.¹⁸ Thus, biomimetic reactions have

inspired us to develop a new H₂O₂ detection method using the iron complex of a fluorophore. Paramagnetic iron in the complex quenched the fluorescence emission of the fluorophore, whereas activation by H₂O₂ triggered intramolecular oxidative cleavage between the iron ionophore and the fluorophore to produce a fluorescence turn-on signal. Oxidative interactions between iron and H₂O₂ have been adopted previously for the fluorescence detection of H₂O₂. In such approaches, aqueous solutions containing a mixture of Fe ions and a fluorescent poly(*p*-phenyleneethynylene) polymer displayed a fluorescence turn-off response in the presence of enzymatically produced H₂O₂.¹⁹ Another recent example is the use of an Fe³⁺ polypyridine complex tethered to dihydroxyphenoxazine, the leuco form of fluorescent resorufin.²⁰ Although the mechanisms have not been fully elucidated, H₂O₂ was proposed to oxidize the Fe center, thereby stimulating the two-electron oxidation of dihydroxyphenoxazine to produce resorufin. This system, however, was sensitive to other reactive oxygen species (ROSS), such as *t*-BuOOH and O₂^{•-}. It should also be noted that iron-based H₂O₂ probes described previously have never been applied to live specimens.

Herein, we report a novel method for the detection of fluorescence in response to the presence of intracellular H₂O₂ (Fig. 1). The probe platform was readily constructed by complexation of iron ions and Zinpyr-1 (ZP1), a fluorescent zinc ion probe,²¹ and this idea might be extended to any ensemble of iron and fluorescent metal ion sensors. We have proposed that the sensing mechanism involves activation of the Fe center by H₂O₂, followed by oxidative *N*-dealkylation of the ligand to liberate the fluorescence-quenching Fe ionophore. The H₂O₂ probe exhibited exceptional selectivity for H₂O₂ over other ROSS, such as •OH, *t*-BuOOH, and O₂^{•-}. Interestingly, the probe localized at the lysosomes of live HeLa cells, producing an organelle-specific response to intracellular H₂O₂.

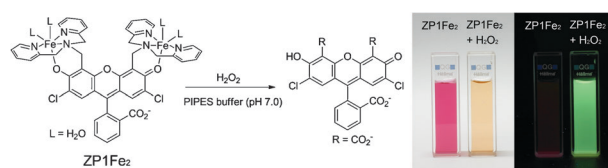


Fig. 1 Structure of the H₂O₂ probe, ZP1Fe₂, and its fluorescence turn-on response. Photographs showing changes in the absorption (left panel; under room light) and fluorescence emission (right panel; under 365 nm UV light) after the addition of H₂O₂.

^a Department of Bioinspired Science, Ewha Womans University, Seoul 120-750, Korea. E-mail: odds2@ewha.ac.kr, wwnam@ewha.ac.kr; Fax: +82-2-3277-4441; Tel: +82-2-3277-2392

^b Division of Life and Pharmaceutical Sciences, Ewha Womans University, Seoul 120-750, Korea

† Electronic supplementary information (ESI) available: Experimental details and more spectroscopic data. CCDC 865223. For ESI and crystallographic data in CIF or other electronic format see DOI: 10.1039/c2cc31632c

The H_2O_2 probe ZP1Fe_2 was prepared by mixing a 20 mM aqueous FeSO_4 solution with a DMSO solution containing 10 mM ZP1. The probe was fully soluble in a pH 7.0 aqueous buffer (25 mM PIPES) and was stable under ambient conditions. The ZP1Fe_2 solution displayed an absorption peak at 507 nm ($\epsilon = 22\,000\ \text{M}^{-1}\ \text{cm}^{-1}$) with a shoulder band around 533 nm in the UV-vis absorption spectrum (ESI†, Fig. S1). The absorption peak was blue-shifted relative to the absorption band of the metal-free form (ZP1; $\lambda_{\text{abs}} = 513\ \text{nm}$). Similarly, the fluorescence emission peak wavelength ($\lambda_{\text{ems}} = 528\ \text{nm}$) for ZP1Fe_2 was blue-shifted relative to ZP1 ($\lambda_{\text{ems}} = 536\ \text{nm}$). ZP1Fe_2 was weakly fluorescent ($\Phi = 0.017$), and fluorescence titration isotherms and Job's plots unambiguously indicated a 1 : 2 binding stoichiometry for ZP1 and Fe complexation (ESI†, Fig. S2). The fluorescence properties were not affected by the presence of biologically relevant metal ions, including Na, Mg, K, Ca, Mn, Ni, Zn, Cu, Cd, and Hg (ESI†, Fig. S3). As expected based on the Irving–Williams series, Cu and Co ions seemed to displace the Fe ions in the ZP1Fe_2 complex, turning off the fluorescence. The fluorescence intensity of ZP1Fe_2 was also resistant to pH changes between 6.25 and 7.81 (ESI†, Fig. S4).

As shown in Fig. 2, addition of an excess of H_2O_2 to a 10 μM ZP1Fe_2 solution provoked fluorescence turn-on at pH 7.0 and 25 °C, with a 22-fold increase in the fluorescence quantum yield ($\Phi = 0.38$). This turn-on ratio is smaller than those of the boronate-based fluorescent H_2O_2 probes,¹² but is still applicable in typical fluorescence microscope experiments. The ZP1Fe_2 fluorescence turn-on response was analyzed by fitting to a pseudo-first order kinetics model, giving a rate constant $k = 0.49 \pm 0.03\ \text{M}^{-1}\ \text{s}^{-1}$ (ESI†, Fig. S5). The limit of detection (LOD) for H_2O_2 was determined to be 29 μM using the three-sigma method. The H_2O_2 probe exhibited exceptional selectivity over other ROSs. As summarized in Fig. 3, almost no response was observed for $\text{O}_2^{\bullet-}$, ^-OCl , $t\text{-BuOOH}$, NO, and $^1\text{O}_2$, and only a small increase in the fluorescence intensity was observed in the cases of $t\text{-BuO}^\bullet$ and $^\bullet\text{OH}$. In addition, chemical oxidants, such as $(\text{NH}_4)_2\text{Ce}^{\text{IV}}(\text{NO}_3)_6$ (CAN) and 2,3-dichloro-5,6-dicyano-*p*-benzoquinone (DDQ), did not produce fluorescence turn on even at concentrations as high as 1 mM. The improved H_2O_2 selectivity suggested that the fluorescence response of ZP1Fe_2 was a consequence of a reaction involving H_2O_2 bound at the iron center rather than other oxidants derived from H_2O_2 (e.g., $^\bullet\text{OH}$). In fact, the fluorescence intensity of 10 μM ZP1Fe_2

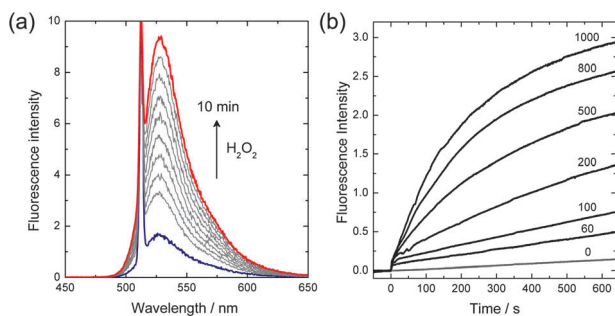


Fig. 2 (a) Fluorescence spectral changes of ZP1Fe_2 (10 μM , PIPES buffer at pH 7.0, 25 °C) after the addition of H_2O_2 (100 equiv.). $\lambda_{\text{ex}} = 512\ \text{nm}$. (b) Time traces of the fluorescence intensity of a ZP1Fe_2 solution observed at 524 nm in the presence of various concentrations of H_2O_2 (0–1000 equiv.).

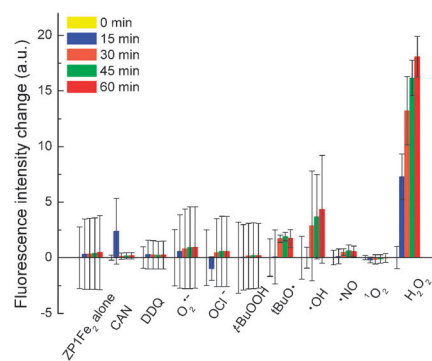


Fig. 3 The selective fluorescence response of ZP1Fe_2 (10 μM) to H_2O_2 relative to other reactive oxygen species ($\text{O}_2^{\bullet-}$, 1 mM KO_2 ; OCl^- , 1 mM NaOCl ; 1 mM $t\text{-BuOOH}$; $t\text{-BuO}^\bullet$, 1 mM FeSO_4 + 100 μM $t\text{-BuOOH}$; $^\bullet\text{OH}$, 1 mM FeSO_4 + 100 μM H_2O_2 ; $^\bullet\text{NO}$, excess NO gas; $^1\text{O}_2$, photosensitization by 1 μM methylene blue)† and chemical oxidants (CAN, 1 mM $(\text{NH}_4)_2\text{Ce}(\text{NO}_3)_6$; DDQ, 1 mM 2,3-dichloro-5,6-dicyano-*p*-benzoquinone). Conditions: $\lambda_{\text{ex}} = 512\ \text{nm}$; pH 7.0 buffer (25 mM PIPES).

did not increase in proportion to the amount of $^\bullet\text{OH}$ present (0–1 mM Fe_2EDTA + 1.5 mM H_2O_2 , pH 7.0 PIPES buffer, 25 °C; ESI†, Fig. S6). Furthermore, the fluorescence intensity of a solution containing 10 μM iron-free ZP1 was not affected by the presence of $^\bullet\text{OH}$ (0–100 μM FeSO_4 + 0–100 mM K_2EDTA + 1.5 mM H_2O_2 , pH 7.0 PIPES buffer, 25 °C; ESI†, Fig. S7). These results led us to exclude the possibility that $^\bullet\text{OH}$ participated in the fluorescence H_2O_2 response of ZP1Fe_2 .

The reaction between ZP1Fe_2 and H_2O_2 produces 2,7-dichloro-fluorescein through dissociation of the Fe ionophores, as evidenced by the identical UV-vis absorption and fluorescence spectra of the product solution and the authentic 2,7-dichloro-fluorescein compound (ESI†, Fig. S8). Since the dinuclear iron centers in ZP1Fe_2 complicated the precise analyses, we synthesized a mononuclear iron complex, 2-((di(2-picolyl)amino)methyl)phenol ([Fe(DPAPhOH)]), as a model compound of ZP1Fe_2 (Fig. 4a). [Fe(DPAPhOH)] displayed an absorption maximum at 512 nm ($\epsilon = 688\ \text{M}^{-1}\ \text{cm}^{-1}$) due to a ligand-to-metal charge-transfer (LMCT) transition between the phenolate and the Fe center.²² Upon addition of 50 equiv. of H_2O_2 , this band disappeared with a rate constant $k = 0.11\ \text{M}^{-1}\ \text{s}^{-1}$ (Fig. 4b), indicating liberation of the phenolate moiety. Cleavage of the phenolate moiety was also observed by ^1H NMR

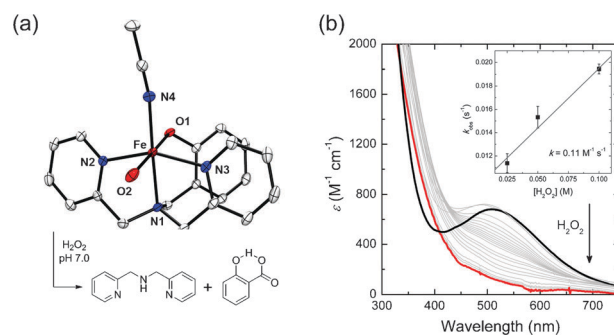


Fig. 4 (a) Crystal structure† (drawn at the 30% probability level) and H_2O_2 -induced cleavage of [Fe(DPAPhOH)]. Hydrogen atoms are omitted for clarity. (b) UV-vis absorption spectra of [Fe(DPAPhOH)] (0.5 mM, pH 7.0 PIPES buffer, 25 °C) after the addition of H_2O_2 (50 equiv.): black, before the addition of H_2O_2 ; red, 10 min after the addition of H_2O_2 .

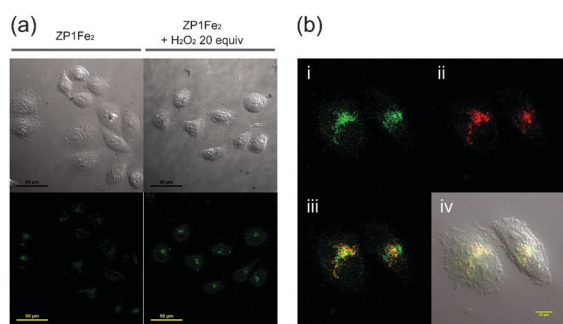


Fig. 5 (a) Fluorescent detection of intracellular H_2O_2 in live HeLa cells: Bright field (top) and fluorescence (bottom) micrographs of HeLa cells incubated with ZP1Fe₂ (10 μM , 30 min). Cells shown in the right panels were treated with H_2O_2 (200 μM , 10 min). Scale bar = 50 μm . (b) Subcellular localized fluorescence signals from the lysosomes. HeLa cells were pretreated with H_2O_2 (200 μM , 10 min) and incubated with ZP1Fe₂ (10 μM , 30 min) and LysoTracker-Red (50 nM, 1 h): (i) ZP1Fe₂ signals; (ii) LysoTracker-Red signals; (iii) merged images (i) and (ii); (iv) bright field image. Scale bar = 10 μm .

(D₂O solution containing 2.5 vol% *d*₆-DMSO) and electro-spray ionization mass spectrometry (ESI[†], Fig. S9 and S10). It is likely that the dissociation proceeded *via* a reactive H_2O_2 adduct of the iron center, such as $\text{Fe}^{\text{III}}\text{-OOH}$ or $\text{Fe}^{\text{IV}}\text{=O}$, similar to the *N*-dealkylation mediated by cytochrome P-450 enzymes.²³ In fact, the formation of a reactive high-spin Fe^{III} species was supported by the observation of a strong EPR signal ($g = 4.30$) in aqueous solutions containing H_2O_2 and [Fe(DPAPHOH)] (ESI[†], Fig. S11).

With an understanding of the fluorescence turn-on response, we evaluated the biological utility of the H_2O_2 probe. ZP1Fe₂ is cell-permeable and nontoxic to live mammalian cells. In fact, MTT assays revealed that the cell viabilities of HeLa cells and COS7 cells were not affected by incubation with 0–20 μM ZP1Fe₂ for 24 h. In contrast, significant cell death was observed when the cells were incubated with 1 μM staurosporine under identical conditions (ESI[†], Fig. S12). Live HeLa cells were therefore incubated with 10 μM ZP1Fe₂ for 30 min, and fluorescence micrographs were taken before and after treatment with 200 μM H_2O_2 . Turn-on fluorescence signals were observed for the HeLa cells treated with H_2O_2 (Fig. 5a). Interestingly, the punctate spots were scattered near the perinuclear regions rather than being evenly distributed in the cytosol. The signal localization was examined by performing colocalization experiments using the live HeLa cells pretreated with 200 μM H_2O_2 , and then incubated with 10 μM ZP1Fe₂ (30 min) and 50 nM LysoTracker-Red (1 h), a lysosome-specific stain. As shown in Fig. 5b, the fluorescence patterns of ZP1Fe₂ and the LysoTracker-Red signals overlapped perfectly, indicating unambiguously that the fluorescence response was localized at the lysosome. Because intracellular H_2O_2 metabolism by lysosomal enzymes is closely linked to oxidative stress,²⁴ the subcellular detection utility of ZP1Fe₂ will be useful in the studies of lysosomal H_2O_2 .

In summary, we developed a new fluorescent probe for H_2O_2 based on the cleavage of the paramagnetic Fe ionophore

from the fluorophore. The unique mechanism affords exceptional selectivity for H_2O_2 over other ROSS. This H_2O_2 probe is applicable to live cell imaging and has the ability to detect intracellular H_2O_2 at the lysosome.

This research was supported by CRI, GRL (2010-00353), and WCU programs (R31-2008-000-10010-0) (W.N.), Basic Science Research Program (2011-0010514) (D.K.), and Ewha Womans University (RP-Grant 2010) (Y.Y.).

Notes and references

† Refer to ESI for a description of the ROSS preparation.

§ Crystal data for [Fe(DPAPHOH)(H₂O)(CH₃CN)](ClO₄)₂: C₂₁H₂₄Cl₂FeN₄O₁₀, monoclinic, *Cc*, *Z* = 4, *a* = 11.3781(2), *b* = 18.5161(3), *c* = 12.4123(2) Å, β = 91.2170(10)°, *V* = 2614.41(8) Å³, ρ_{calcd} = 1.573 g cm⁻³, *m* = 0.842 mm⁻¹, *R*₁ = 0.0304, *wR*₂ = 0.0802, *GOF* = 0.913 for 5695 unique reflections and 356 variables. Flack parameter = -0.001(11). The crystallographic data for [Fe(DPAPHOH)(H₂O)(CH₃CN)](ClO₄)₂ are listed in ESI, Table S1, and Table S2 lists the selected bond distances and angles. CCDC 865223 for [Fe(DPAPHOH)(H₂O)(CH₃CN)](ClO₄)₂ contains the supplementary crystallographic data associated with this paper.

- R. S. Balaban, S. Nemoto and T. Finkel, *Cell*, 2005, **120**, 483–495.
- S. G. Rhee, *Science*, 2006, **312**, 1882–1883.
- H. A. Woo, S. H. Yim, D. H. Shin, D. Kang, D.-Y. Yu and S. G. Rhee, *Cell*, 2010, **140**, 517–528.
- J. D. Lambeth, *Nat. Rev. Immunol.*, 2004, **4**, 181–189.
- N. Soh, *Anal. Bioanal. Chem.*, 2006, **386**, 532–543.
- X. Chen, X. Tian, I. Shin and J. Yoon, *Chem. Soc. Rev.*, 2011, **40**, 4783–4804.
- M. Schäferling, D. B. M. Grögel and S. Schreml, *Microchim. Acta*, 2011, **174**, 1–18.
- N. Soh, O. Sakawaki, K. Makihara, Y. Odo, T. Fukaminato, T. Kawai, M. Irie and T. Imato, *Bioorg. Med. Chem.*, 2005, **13**, 1131–1139.
- S. L. Hempel, G. R. Buettner, Y. Q. O'Malley, D. A. Wessels and D. M. Flaherty, *Free Radical Biol. Med.*, 1999, **27**, 146–159.
- A. Negre-Salvayre, N. Augé, C. Duval, F. Robbesyn, J.-C. Thiers, D. Nazzari, H. Benoist and R. Salvayre, *Methods Enzymol.*, 2002, **352**, 62–71.
- M. Zhou, Z. Diwu, N. Panchuk-Voloshina and R. P. Haugland, *Anal. Biochem.*, 1997, **253**, 162–168.
- A. R. Lippert, G. C. Van de Bittner and C. J. Chang, *Acc. Chem. Res.*, 2011, **44**, 793–804.
- H. Maeda, Y. Fukuyasu, S. Yoshida, M. Fukuda, K. Saeki, H. Matsuno, Y. Yamauchi, K. Yoshida, K. Hirata and K. Miyamoto, *Angew. Chem., Int. Ed.*, 2004, **43**, 2389–2391.
- K. Xu, B. Tang, H. Huang, G. Yang, Z. Chen, P. Li and L. An, *Chem. Commun.*, 2005, 5974–5976.
- M. Abo, Y. Urano, K. Hanaoka, T. Terai, T. Komatsu and T. Nagano, *J. Am. Chem. Soc.*, 2011, **133**, 10629–10637.
- K.-i. Setsukinai, Y. Urano, K. Kakinuma, H. J. Majima and T. Nagano, *J. Biol. Chem.*, 2003, **278**, 3170–3175.
- O. S. Wolfbeis, A. Duerkop, M. Wu and Z. Lin, *Angew. Chem., Int. Ed.*, 2002, **41**, 4495–4498.
- G. Battistuzzi, M. Bellei, C. A. Bortolotti and M. Sola, *Arch. Biochem. Biophys.*, 2010, **500**, 21–36.
- T. Zhang, H. Fan, G. Liu, J. Jiang, J. Zhou and Q. Jin, *Chem. Commun.*, 2008, 5414–5416.
- Y. Hitomi, T. Takeyasu, T. Funabiki and M. Kodera, *Anal. Chem.*, 2011, **83**, 9213–9316.
- G. K. Walkup, S. C. Burdette, S. J. Lippard and R. Y. Tsien, *J. Am. Chem. Soc.*, 2000, **122**, 5644–5645.
- Y. Nishida, H. Shimo and S. Kida, *J. Chem. Soc., Chem. Commun.*, 1984, 1611–1612.
- F. P. Guengerich and T. L. Macdonald, *Acc. Chem. Res.*, 1984, **17**, 9–16.
- T. Kurz, A. Terman, B. Gustafsson and U. T. Brunk, *Biochim. Biophys. Acta, Gen. Subj.*, 2008, **1780**, 1291–1303.